1874-1290/19 *Send Orders for Reprints to reprints@benthamscience.net*

19

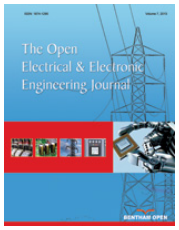

The Open Electrical & Electronic Engineering Journal

Content list available at: https://openelectricalandelectronicengineeringjournal.com

RESEARCH ARTICLE

Non-redundant Spherical Near-Field to Far-Field Transformation for a Volumetric Antenna in Offset Configuration

Francesco D'Agostino, Flaminio Ferrara, Claudio Gennarelli*, Rocco Guerriero and Massimo Migliozzi

Department of Industrial Engineering - University of Salerno, Fisciano, Italy

Abstract:

Background:

The development of fast Near-Field (NF) measurement techniques allowing the precise determination of the Far-Field (FF) radiation features of an antenna is becoming more and more challenging nowadays.

Objective:

The goal of the article is the development of an NF To FF Transformation (NFTFFT) with spherical scan for offset mounted volumetric Antennas Under Tests (AUTs) requiring, unlike the classical technique, a reduced set of NF data, that is of the same amount as for the onset mounting case, thus making data gathering faster. In fact, the number of NF data needed by the standard approach may considerably increase in this case, since the size of the smallest sphere surrounding the AUT and centered at the center of the measurement sphere rises.

Methods:

This goal has been achieved by profitably exploiting the non-redundant sampling representation of electromagnetic field and assuming a volumetric AUT as contained in a sphere. An optimal sampling interpolation algorithm is then employed to precisely reconstruct the input NF data for the traditional spherical NFTFFT from the reduced set of the collected ones.

Conclusion:

The numerical simulations and experimental tests demonstrate the effectiveness of the developed approach accounting for an offset mounting of the AUT.

Keywords: Antenna measurements, Non-redundant sampling representations of electromagnetic fields, Spherical scanning, Offset mounting, Near-field to far-field transformations, FF region, EM Field.

Article History	Received: October 08, 2018	Revised: November 25, 2018	Accepted: December 31, 2018

1. INTRODUCTION

Near-Field To Far-Field Transformation (NFTFFT) techniques [1 - 6] have become in the last years an increasingly recognized and used tool to precisely determine the radiation features of antennas whose dimensions are large in terms of wavelength. As a matter of fact, the precise characterization of an antenna must be performed in its FF region and in a controlled environment, such as an anechoic chamber, where the free-space propagation condition is well approximated by making negligible the field reflections from the walls, as well as the Electromagnetic (EM) interferences from external sources. Accordingly, since the FF requirements cannot be met in an anechoic chamber for Antennas Under Test (AUTs) having large or even medium electrical dimensions, only NF measurements are possible in such a case and the AUT radiation pattern must be evaluated by means of a suitable NFTFFT technique. These techniques typically consider the AUT radiated EM field as summation of modes, which are elementary solutions of the vector wave equation in a free sources region. The required modal coefficients, which allow a precise recovery of the antenna radiated far field once substituted in the corresponding expansion valid in the FF region, can be evaluated from the magnitude and phase measurements of the voltage acquired by the probe in two its different orientations on a proper grid of the scanning surface. The NFTFFT using the spherical scan is undoubtedly the most appealing one, because it allows one to reconstruct the whole

* Address correspondence to this author at the Department of Industrial Engineering - University of Salerno; *via* Giovanni Paolo II, 132 - 84084 Fisciano (SA) Italy; E-mail: cgennarelli@unisa.it

FF pattern of the AUT avoiding the errors caused by the truncation of the measurement area. Accordingly, it has caught large attention from the antenna measurement community, as attested by the numerous research papers [7 - 20] dealing with such a topic.

The spatially quasi-band limitation properties of the EM fields scattered by finite sizes targets or radiated by antennas [21] have been suitably exploited in [10] to optimize the Classical Spherical (CS) NFTFFT [9], by showing that the sampling rate on the scanning parallels decreases when approaching the poles. Moreover, it has been possible to rigorously relate the maximum order of the spherical wave expansion of the AUT field to its spatial bandwidth and not just according to the empirical rule based on the radius of the smallest sphere surrounding the antenna. In the same paper, the Non-Redundant (NR) sampling representations of the EM field [22, 23] have been profitably employed to develop efficient NR NFTFFTs, requiring a number of NF measurements remarkably smaller than that used by the CS NFTFFT [9] when dealing with long or quasi-planar AUTs, modelled as enclosed in a prolate or oblate spheroid. In fact, the NF data required to execute the CS NFTFFT [9] are precisely reconstructed from the collected NR ones, *via* optimal sampling interpolation (OSI) formulas [24]. The so obtained remarkable reduction in the number of needed NF data leads to a considerable measurement time-saving, which is a very significant result, because the measurement time is greater and greater with respect to that required to perform the NFTFFT. Indeed, the NR NFTFFTs [10] considered an ideal probe and, therefore, did not account for the effects related to the use of a real probe. Probe compensated NR NFTFFTs for long or quasi-planar AUTs, assumed as contained in a cylinder terminated by two spherical caps or in two circular bowls with equal aperture radii, have been developed in [13] when adopting a non-directive probe. As a matter of fact, it has been proved [25] that the voltage detected by this type of probe exhibits practically the same spatial bandwidth of the EM field radiated by the AUT and, thus, the results in [22, 23] can be utilized to achieve an NR representation of such a voltage too. At last, the NR NFTFFTs [13] and the probe compensated version of those in [10] have been experimentally assessed in [17] and [16] respectively.

However, particular disposals of the antenna on the mounting supports, mechanical limitations of the AUT positioners or their special arrangements, may prevent the possibility of a mounting wherein the AUT and scanning sphere centres coincide (onset AUT mounting) [26]. In such a case, according to the empirical rule based on the minimum sphere, the amount of the NF measurements required by the CS NFTFFT [9], as well as the corresponding acquisition time, can considerably increase because of the growth of the radius of the smallest sphere surrounding the AUT with its centre at the measurement sphere one. For overcoming such an issue, Foged *et al*., developed in [26] a new spherical NFTFFT for AUTs mounted in offset (non-centered) configuration, where the spherical wave expansion (SWE) functions are formulated with respect to the AUT centre rather than to the scan sphere one. Even if the number of required NF data is, in this case, considerably smaller than that set by the empirical rule, it remains a bit larger than that relevant to an AUT mounting in onset (centered) configuration [26].

The goal of this article is to develop and assess, both numerically and experimentally, an effective NR NFTFFT with a spherical scan for offset mounted volumetric antennas, requiring the same amount of NF measurements in both the cases of offset and onset AUT mountings. As it will be shown, when dealing with an offset AUT mounting, such a number results to be remarkably smaller than that set by the minimum sphere rule when applying the CS NFTFFT [9].

The paper is organized as follows: An NR sampling representation of the probe voltage on a scanning sphere, accounting for an AUT mounted in an offset configuration, is presented in Sect. 2. The numerical and experimental assessments of the developed NR sampling representation are provided in Sects. 3 and 4, respectively. Conclusions and further remarks are then drawn in Sect. 5.

2. NR PROBE VOLTAGE REPRESENTATION ON A SPHERE FOR A VOLUMETRIC AUT IN OFFSET CONFIGURATION

Let us tackle the following problem: to develop an NR sampling representation of the voltage detected at the terminals of a non-directive probe when a quasi-spherical AUT, to be measured in a spherical NF system, cannot be mounted in onset configuration for practical constraints. To this end, let us introduce two spherical reference systems. The former, $S(r,\vartheta,\varphi)$, has its origin O at the centre of the measurement sphere of radius d and is used for denoting any observation point P. The latter, $S'(r',\vartheta',\varphi')$, with its origin O' at the antenna centre, which is assumed to lie on the z axis at distance d_s from O, and its z' axis coincident with the z one (Fig. **1**), properly accounts for the offset AUT mounting and is used for developing an actually non-redundant sampling representation. In fact, according to [22], the number of required samples is minimized by reducing as much as possible the area of the convex rotational surface Σ containing the AUT. Thus, the NR representation in S' of the voltage measured by a non-directive probe over each of the curves Γ (meridian curves and azimuthal circumferences), describing the spherical measurement surface, can be attained [22, 23]: i) by modelling the considered AUT exhibiting a quasi-spherical shape as contained in the smallest sphere Σ of radius a; ii) by adopting a suitable parameter η to represent Γ; iii) by defining the "reduced voltage".

$$\tilde{V}(\eta) = \exp\left[\mathrm{j}\psi(\eta)\right]V(\eta) \qquad (1)$$

where $V(\eta)$ is the voltage revealed by the probe (V_p) or by the probe rotated by 90° around its axis (V_r) and $\exp[\mathrm{j}\Psi(\eta)]$ a proper phase factor. Now, the so obtained $\tilde{V}(\eta)$ is a spatially quasi-bandlimited function and can be closely approximated by a function spatially bandlimited to $\chi' W_\eta$, where W_η is a critical value [22] and χ' an excess bandwidth factor to be suitably chosen to control the corresponding band limitation error [22].

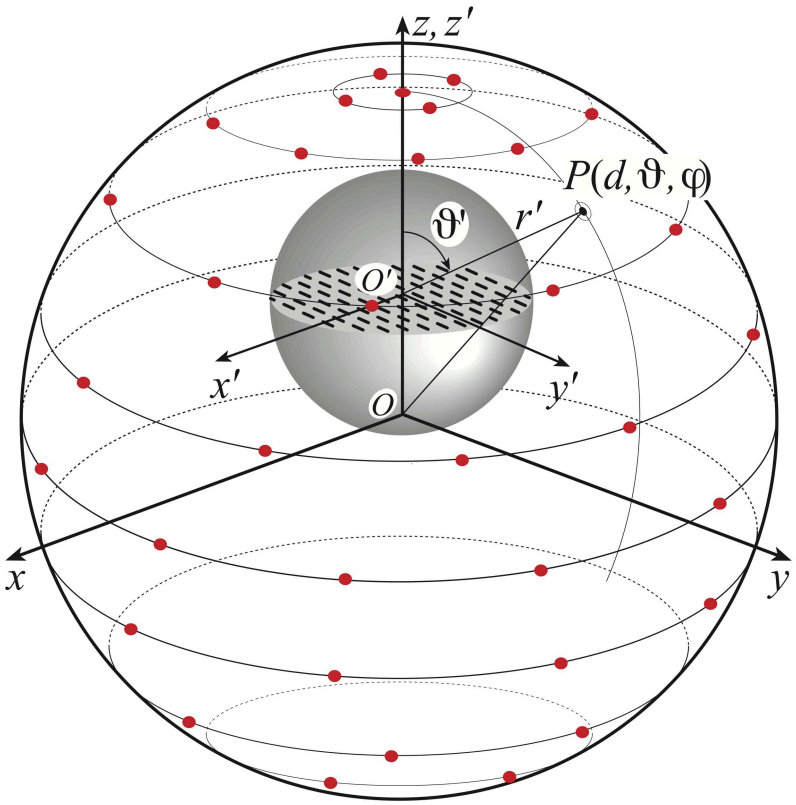

Fig. (1). Spherical scan for a volumetric AUT in offset mounting.

The spatial bandwidth W_η, the optimal parameter η, and the corresponding phase factor $\exp[j\Psi(\eta)]$, when Γ coincides with a meridian curve, are [22]:

$$W_\eta = \beta a \; ; \qquad \eta = \vartheta' \; ;$$
$$\exp[j\psi(\eta)] = \exp\left[j\beta\sqrt{r'^2 - a^2} - \beta a \cos^{-1}(a/r')\right] \tag{2}$$

where $\beta = 2\pi/\lambda$ is the free-space wavenumber, with λ being the related wavelength.

When Γ is an azimuthal circumference, the phase factor $\exp[j\Psi(\eta)]$ is constant owing to the rotational symmetry and the angle φ' can be suitably used as optimal parameter η [22]. As shown in [22], the corresponding bandwidth is, in such a case, given by:

$$W_{\varphi'}(\vartheta') = \beta a \sin\vartheta' \tag{3}$$

According to the above achievements, the complex voltage value at a generic observation point P on the meridian curve at φ' can be determined in a fast and efficient way through the following OSI formula [22]

$$V(\eta(\vartheta'), \varphi') = \exp[-j\psi(\eta)] \sum_{n=n_0-q+1}^{n_0+q} \tilde{V}(\eta_n, \varphi')\, \Omega_N(\eta - \eta_n, \bar{\eta})\, D_{N''}(\eta - \eta_n) \tag{4}$$

from the intermediate reduced voltage samples $\tilde{V}(\eta_n, \varphi')$, namely the reduced voltages at the intersections between the considered meridian curve and the sampling azimuthal circumferences. In (4), $2q$ is the number of the considered nearest intermediate samples, $n_0 = \mathrm{Int}(\eta/\Delta\eta)$, is the index of the sample nearest (on the left) to the point P, Int(x) stays for the integer part of x, and

$$\Omega_N(\eta, \bar{\eta}) = \frac{T_N\left[2\cos^2(\eta/2)/\cos^2(\bar{\eta}/2) - 1\right]}{T_N\left[2/\cos^2(\bar{\eta}/2) - 1\right]};$$
$$D_{N''}(\eta) = \frac{\sin[(2N''+1)\eta/2]}{(2N''+1)\sin(\eta/2)} \tag{5}$$

are the Tschebyscheff and Dirichlet sampling functions, $T_N(\eta)$ being the N degree Tschebyscheff polynomial. Moreover,

$$\eta_n = n\Delta\eta = 2\pi n/(2N''+1); \qquad N'' = \mathrm{Int}(\chi N') + 1 \tag{6}$$

$$N' = \mathrm{Int}(\chi' W_\eta) + 1; \; N = N'' - N'; \qquad \bar{\eta} = q\Delta\eta \tag{7}$$

where $\chi > 1$ is an oversampling factor to be used in the OSI expansion in order to control the truncation error.

The intermediate samples are accurately determined [22] by interpolating the reduced voltage samples $\tilde{V}(\eta_n, \varphi'_{m,n})$ on the sampling azimuthal circumferences fixed by η_n values *via* the OSI expansion:

$$\tilde{V}(\eta_n, \varphi') = \sum_{m=m_0-p+1}^{m_0+p} \tilde{V}(\eta_n, \varphi'_{m,n})\, \Omega_{M_n}(\varphi' - \varphi'_{m,n}, \bar{\varphi}')\, D_{M''_n}(\varphi' - \varphi'_{m,n}) \quad (8)$$

where $2p$ is the considered nearby samples number, $m_0 = \mathrm{Int}(\varphi'/\Delta\varphi'_n)$, and

$$\varphi'_{m,n} = m\Delta\varphi'_n = 2\pi m/(2M''_n+1)\,; \quad M''_n = \mathrm{Int}(\chi M'_n) + 1 \quad (9)$$

$$M'_n = \mathrm{Int}\left[\chi^* \beta a \sin\vartheta'(\eta_n)\right] + 1\,; \quad M_n = M''_n - M'_n \quad (10)$$

$$\chi^* = (\chi' - 1)\left[\sin\vartheta'(\eta_n)\right]^{-2/3} + 1\,; \quad \bar{\varphi}' = p\Delta\varphi'_n \quad (11)$$

It can be useful to stress that the dependence of the azimuthal excess bandwidth factor χ^* on $\vartheta'(\eta_n)$ is necessary to assure practically the same bandlimitation error on all the sampling azimuthal circumferences [21].

By substituting relation (8) into (4), the sought two-dimensional OSI formula is finally attained:

$$V(\eta(\vartheta'), \varphi') = \exp[-\mathrm{j}\psi(\eta)] \sum_{n=n_0-q+1}^{n_0+q} \left\{ \Omega_N(\eta - \eta_n, \bar{\eta})\, D_{N''}(\eta - \eta_n) \cdot \sum_{m=m_0-p+1}^{m_0+p} \tilde{V}(\eta_n, \varphi'_{m,n})\, \Omega_{M_n}(\varphi' - \varphi'_{m,n}, \bar{\varphi}')\, D_{M''_n}(\varphi' - \varphi'_{m,n}) \right\} \quad (12)$$

In order to apply the above two-dimensional OSI formula to accurately recover, from the acquired NR samples, the voltages V_p and V_r of the probe and rotated probe at the positions on the scanning sphere specified by the CS NFTFFT [9] or by its version as rearranged in [10, 13], the following points must be stressed: i) the coordinates of the sampling points on the scan sphere are set by the proposed NR sampling representation in the reference frame, S' but have to be determined in the S one to drive the positioner controllers at the acquisition stage; ii) the positions of the input NF data for the NFTFFT are, obviously, given in S, but have to be expressed in S' to execute the interpolation. It is a simple task to verify that the relations linking the coordinates of S and S' are:

$$\varphi = \varphi'\,; \quad \vartheta = \tan^{-1}[r'\sin\vartheta'/(r'\cos\vartheta' + d_S)] \quad (13)$$

$$\vartheta' = \tan^{-1}[d\sin\vartheta/(d\cos\vartheta - d_S)]\,; \quad r' = -d_S\cos\vartheta' + \sqrt{d^2 - (d_S\sin\vartheta')^2} \quad (14)$$

3. NUMERICAL TESTING

The efficacy of the proposed NR NFTFFT with spherical scan for volumetric AUTs mounted in offset configuration has been demonstrated by several simulations. In the here shown ones, the measurement sphere has radius d = 32 λ and the considered AUT is a uniform planar array at $z = d_s$ = 11λ, lying on a circle with diameter $2a$ = 31 λ. The array elements, elementary Huygens sources linearly polarized along *y,* are symmetrically placed with respect to the x = 0 plane and are spaced by 0.5 λ both radially and azimuthally. A sphere with radius a = 15.5 λ and centred in O', of Cartesian coordinates (0, 0, 11 λ) in S, has been chosen as surface Σ containing the AUT. Moreover, the considered scanning probe, acquiring the voltages V_p and V_r, is an open-ended WR90 rectangular waveguide.

Typical examples of reconstruction of the magnitude and phase of the voltage V_r relevant to the cut plane at φ = 90° are reported in Figs. (**2** and **3**). For reader's convenience, the reconstructions of the magnitudes of V_p and V_r on the cut plane at φ = 30° are displayed in Fig. (**4**) too. As can be observed, the exact voltages and those reconstructed from their NR samples are practically identical.

The accuracy of the two-dimensional OSI expansion (12) is assessed more quantitatively by the curves of the normalized mean-square errors relevant to the reconstruction of V_r shown in Fig. (**5**) for χ' = 1.20, $q = p$ spanning from 3 to 12, and χ = 1.10,1.15,1.20,1.25. These curves have been attained by comparing the voltage values determined from the NR samples *via* (12) and the exact ones on a spherical grid with a 1° step along ϑ and φ. As can be noticed, very low error values are obtained when the oversampling factor and/or the number of the nearby considered samples are increased. The robustness of the OSI formula (12), namely its stability towards random errors which unavoidably affect the NF measurements, has been proved too. To this end, the exact samples have been corrupted with random errors, simulating a random uncertainty on the samples magnitude and phase, uniformly distributed in $[-\Delta a_r, \Delta a_r]$ and in $[-\Delta\alpha_r, \Delta\alpha_r]$, respectively. Moreover, the presence of an environmental noise having magnitude bounded to Δa and random phase has been also considered. As it clearly appears from Fig. (**6**), the proposed OSI expansion results to be robust, thus demonstrating its applicability from the practical viewpoint.

Finally, the two-dimensional OSI formula (12) has been used to evaluate the NF data necessary to perform the CS NFTFFT as rearranged in [10, 13]. The so obtained E-plane radiation pattern is compared with the exact one in Fig. (**7**). As it can be clearly observed, this pattern and the exact one overlap perfectly, thus thoroughly assessing the efficacy of the presented NR NFTFFT with spherical scanning for volumetric AUTs mounted in offset configuration.

For sake of comparison, it must be highlighted that the number of utilized NR NF samples is 26978, considerably

smaller than that (130562) needed by the CS NFTFFT [9] for satisfying the minimum sphere radius rule, as well as smaller than that necessary for applying the approach recently proposed in [26], using an amount of NF data a bit larger than that (32514) necessary for the CS NFTFFT in the onset mounting case.

4. EXPERIMENTAL VERIFICATION

The developed NR spherical NFTFFT for offset mounted volumetric AUTs has been also validated through experimental proofs carried out *via* the roll (φ axis) over azimuth (ϑ axis) spherical NF measurement facility Fig. (**8**), which is present in the anechoic chamber of the antenna measurements laboratory of the University of Salerno and is realized by mounting the probe on a linear vertical positioner and the AUT on a rotator. The rotator, allowing the change of the angle φ, is attached to an L-shaped bracket, mounted on a rotating table which instead allows to vary the angle ϑ. As can be seen in Fig. (**8**), such a rotating table is covered by absorbers to avoid a decay of the anechoic chamber's performances, and the vertical scanner is used only to align the probe and the AUT. The anechoic chamber walls are covered by pyramidal absorbers assuring a reflection level less than -40 dB. The measurements of magnitude and phase of the probe voltages V_p and V_r, collected by an open-ended WR-90 rectangular waveguide over a spherical scanning surface of radius d = 66.4 cm, have been accomplished *via* an Anritsu VNA. An X-band flat plate slotted array at 9.3 GHz, manufactured by Rantec Microwave Systems Inc., having a quasi-circular profile with radius of about 23 cm, has been employed as AUT (Fig. **8**). Its aperture is located on the plane z = 37 cm with the centre O' on the z axis, thus simulating a situation wherein it is not possible a mounting of the AUT in onset configuration owing to practical limitations. As described in Sect. 2, the NR sampling representation in the reference frame S' for the probe voltages V_p and V_r on the scanning sphere has been got by modelling such an AUT as contained in a sphere of radius a = 23.1 cm.

Figs. (**9** and **10**) show the comparison between the magnitude and phase of V_r relevant to the cut plane at φ = 0° evaluated from the NR samples by applying (12) and the directly measured ones, whereas Figs. (**11** and **12**) report the analogous comparisons relevant to V_p on the cut plane at φ = 90°. The reconstruction of the magnitude of V_r relevant to the cut plane at φ = 45° is displayed in Fig. (**13**) for completeness. As it can be clearly observed, a very good agreement results. It should be also noted (Fig. **14**) the slower behaviour of the magnitudes of the reconstructed voltages, in which the fast ripple present in the directly measured ones and caused by the residual reflections from the walls, ceiling, and floor of the anechoic chamber is filtered. This behaviour is imputable to the low pass filtering features of the OSI functions, which are able to cut away the spatial harmonics of the noise greater than the spatial bandwidth of the AUT. It is noteworthy that the above recoveries have been attained by choosing $\chi = \chi' = 1.20$ and $p = q$ = 7, which, according to the results of previous section, guarantee a level of the reconstruction error lower than that relevant to the measurement error.

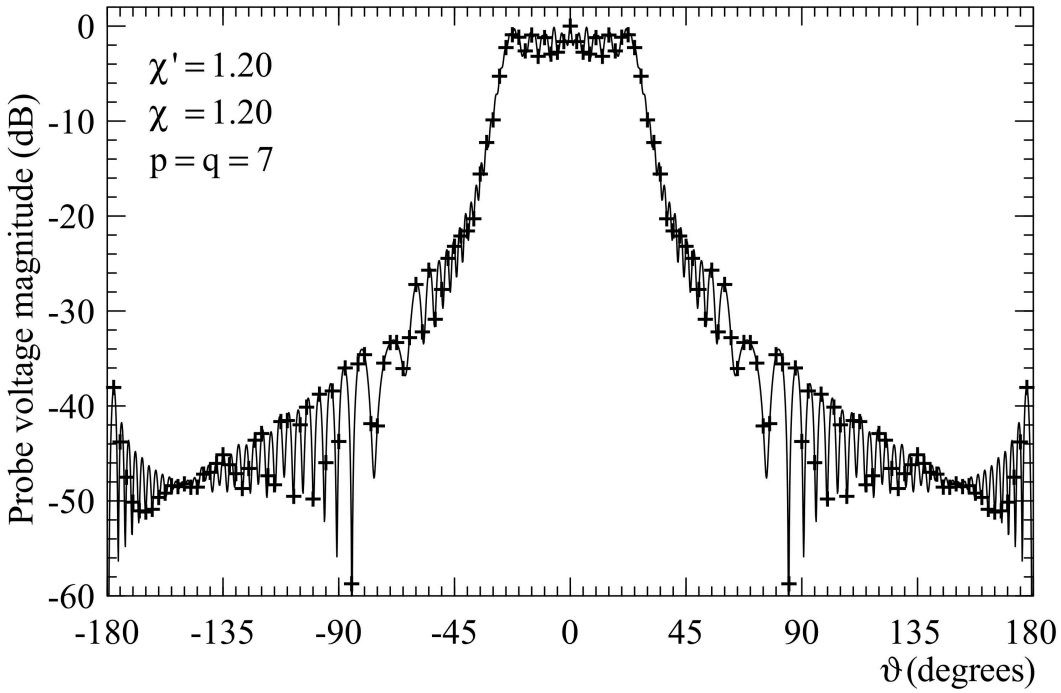

Fig. (2). Magnitude of V_r on the cut plane @ φ = 90°. Solid line: exact. Crosses: evaluated from the NR NF samples.

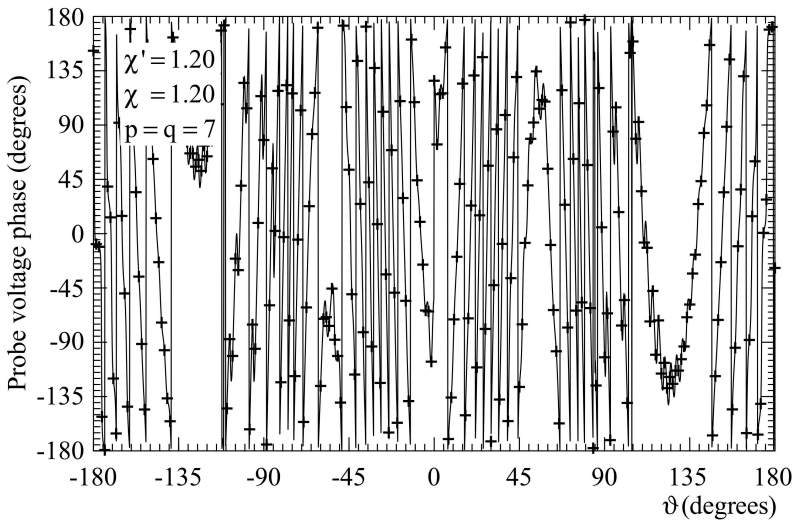

Fig. (3). Phase of V_r on the cut plane @ $\varphi = 90°$. Solid line: exact. Crosses: evaluated from the NR NF samples.

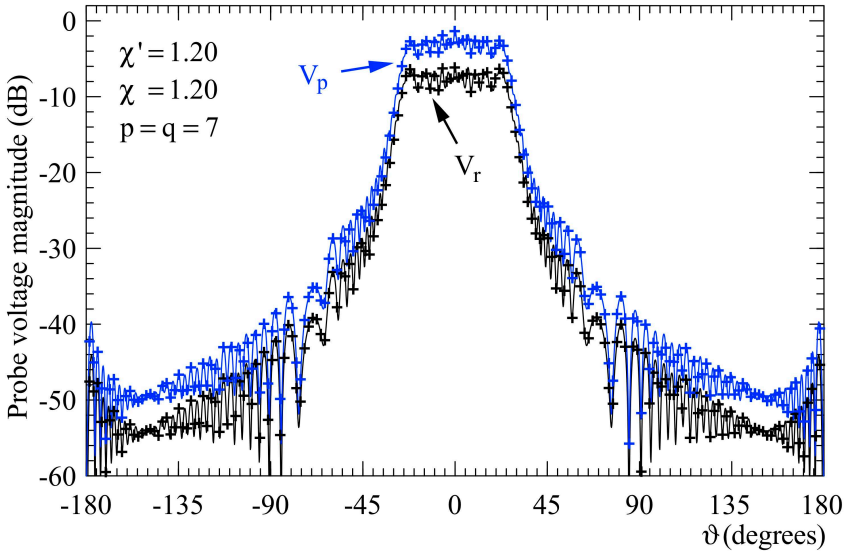

Fig. (4). Magnitudes of V_p and V_r on the cut plane @ $\varphi = 30°$. Solid lines: exact. Crosses: evaluated from the NR NF samples.

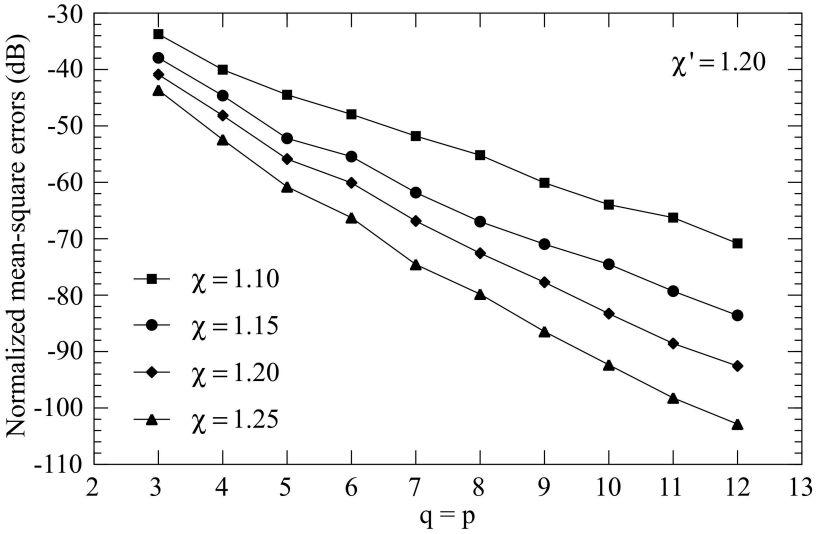

Fig. (5). Normalized mean-square errors relevant to the reconstruction of V_r.

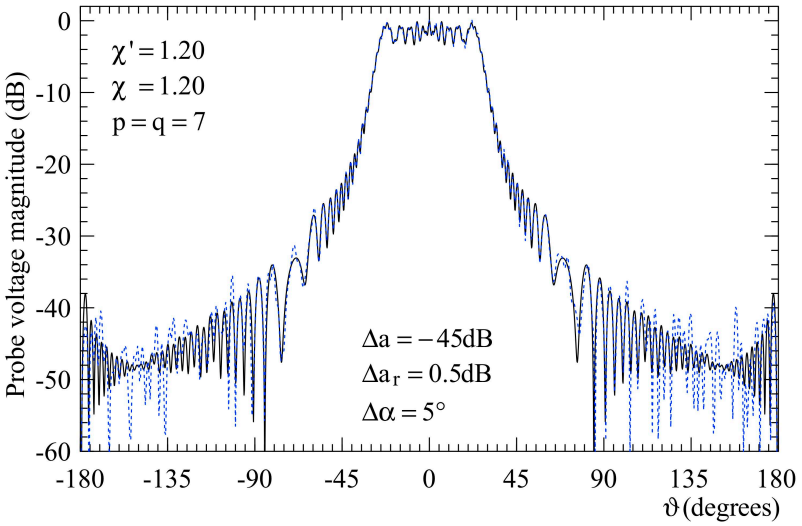

Fig. (6). Magnitude of V_r on the cut plane @ $\varphi = 90°$. Solid line: exact. Dashed line: evaluated from the error affected NR NF samples.

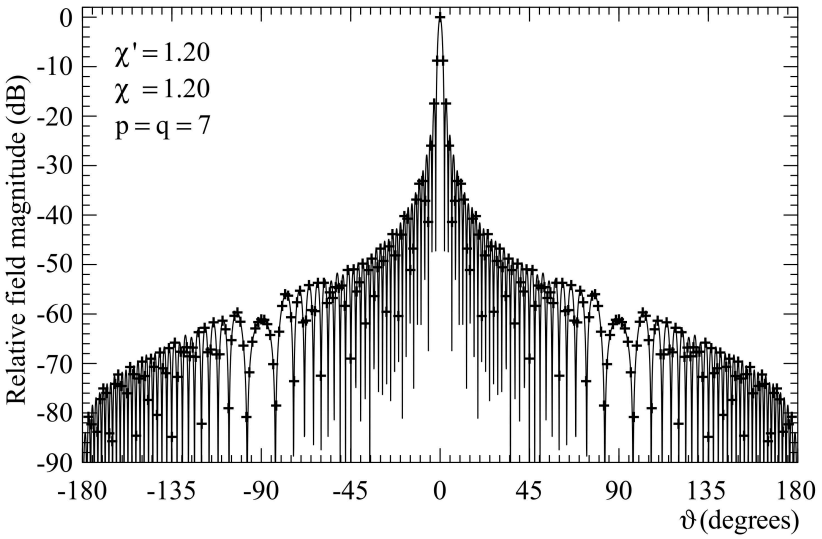

Fig. (7). E-plane pattern. Solid line: exact. Crosses: evaluated from the NR NF samples.

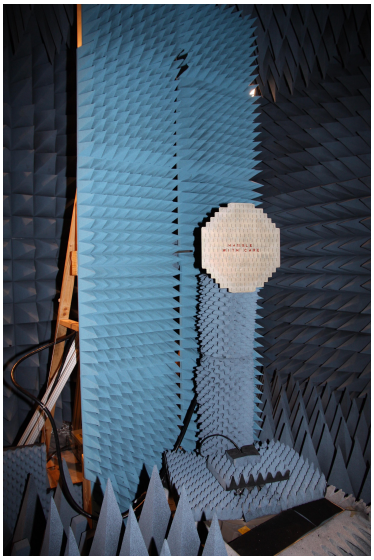

Fig. (8). Photo of the Rantec antenna in the spherical NF facility available at the University of Salerno.

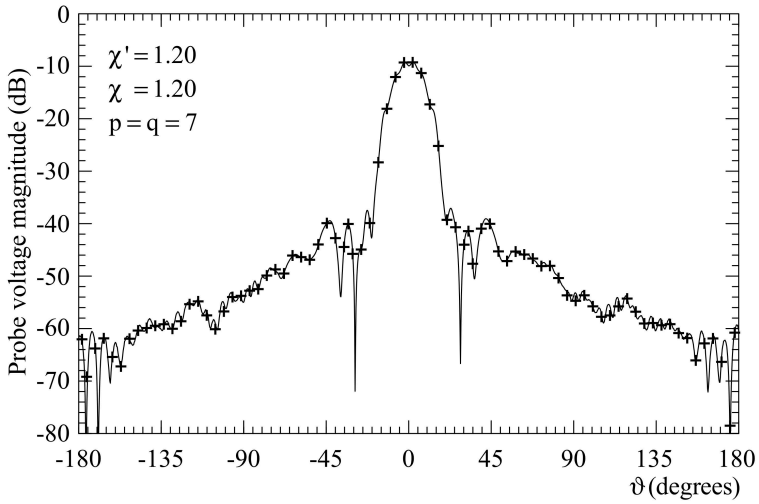

Fig. (9). Magnitude of V_r on the cut plane @ $\varphi = 0°$. Solid line: measured. Crosses: evaluated from the acquired NR NF samples.

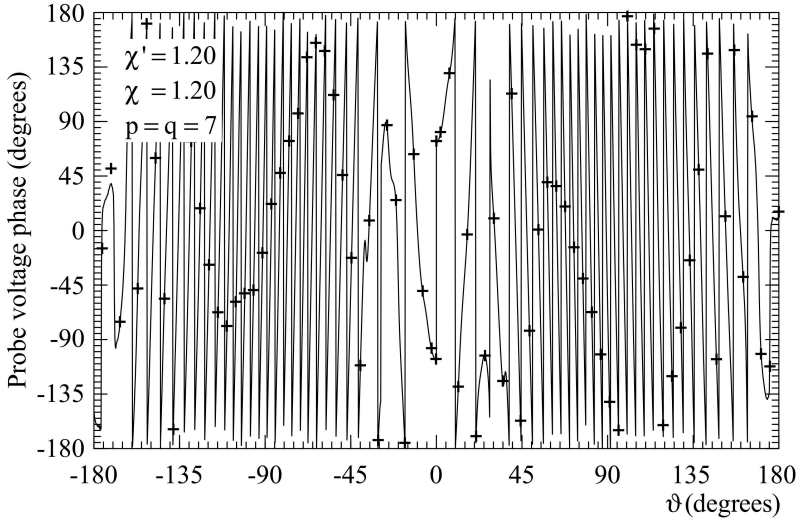

Fig. (10). Phase of V_r on the cut plane @ $\varphi = 0°$. Solid line: measured. Crosses: evaluated from the acquired NR NF samples.

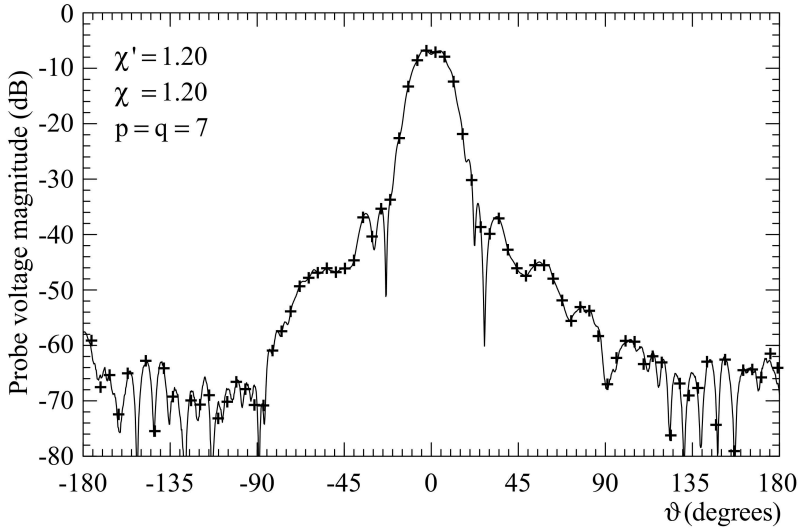

Fig. (11). Magnitude of V_p on the cut plane @ $\varphi = 90°$. Solid line: measured. Crosses: evaluated from the acquired NR NF samples.

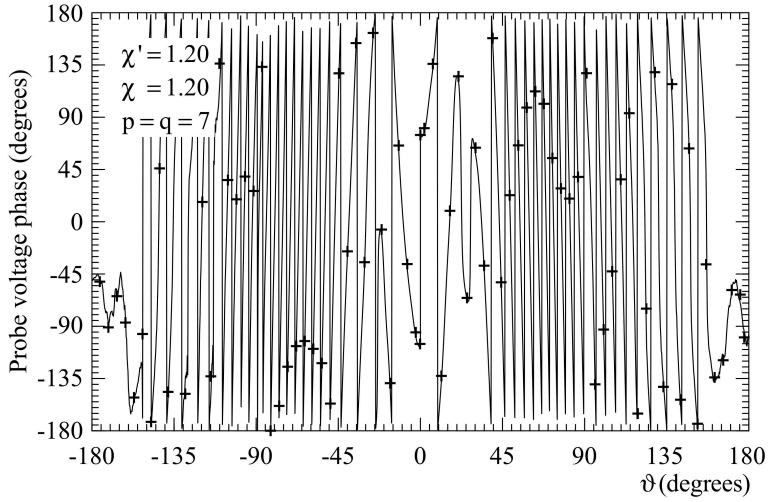

Fig. (12). Phase of V_p on the cut plane @ $\varphi = 90°$. Solid line: measured. Crosses: evaluated from the acquired NR NF samples.

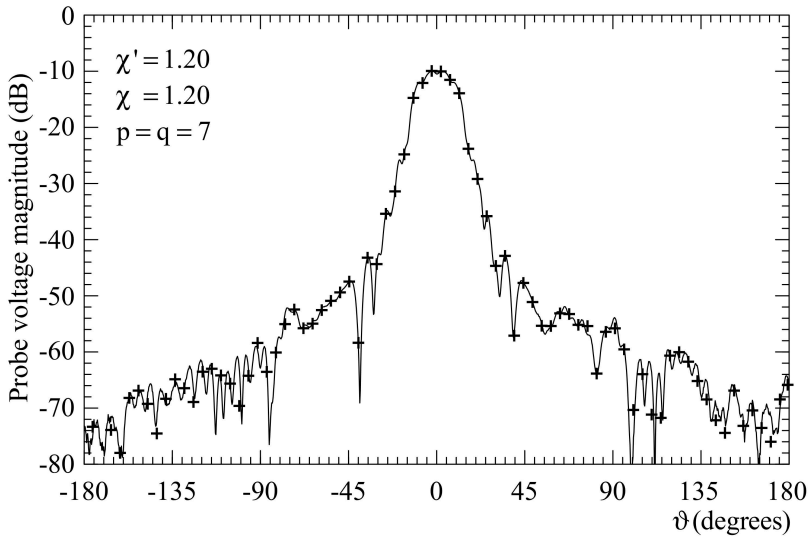

Fig. (13). Magnitude of V_r on the cut plane @ $\varphi = 45°$. Solid line: measured. Crosses: evaluated from the acquired NR NF samples.

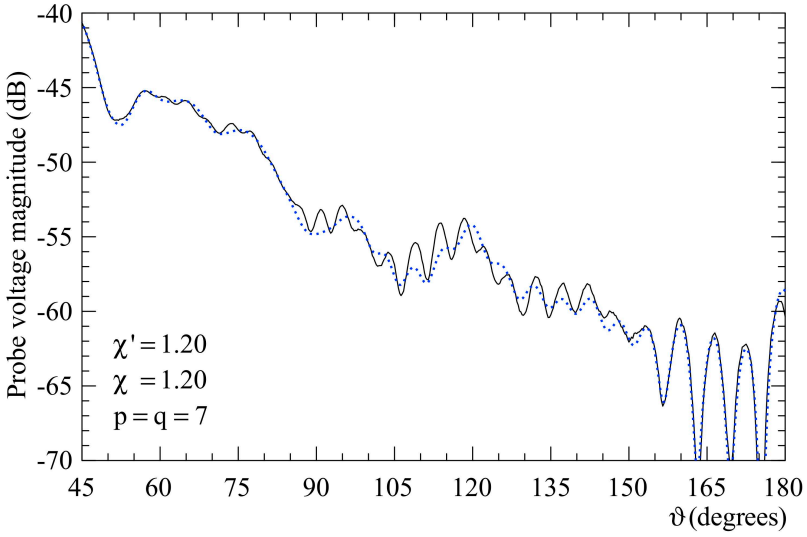

Fig. (14). Magnitude of V_r on the cut plane @ $\varphi = 0°$. Solid line: measured. Dashed line: evaluated from the acquired NR NF samples.

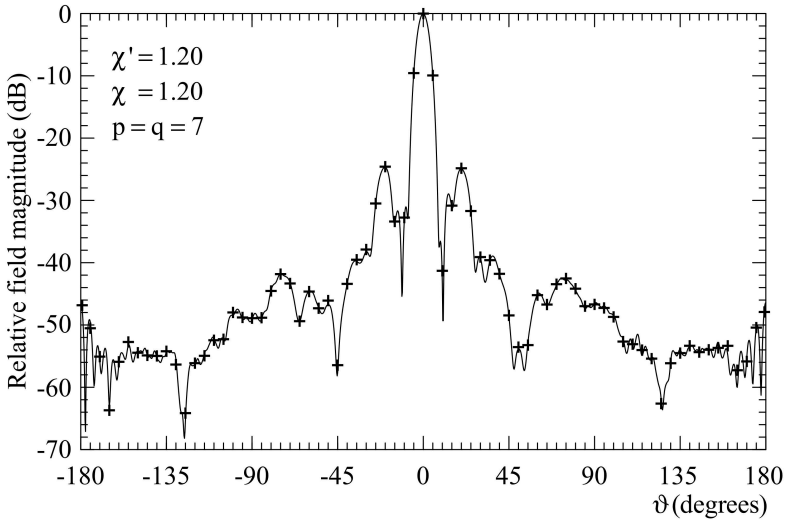

Fig. (15). E-plane pattern. Solid line: reference. Crosses: evaluated from the acquired NR NF samples.

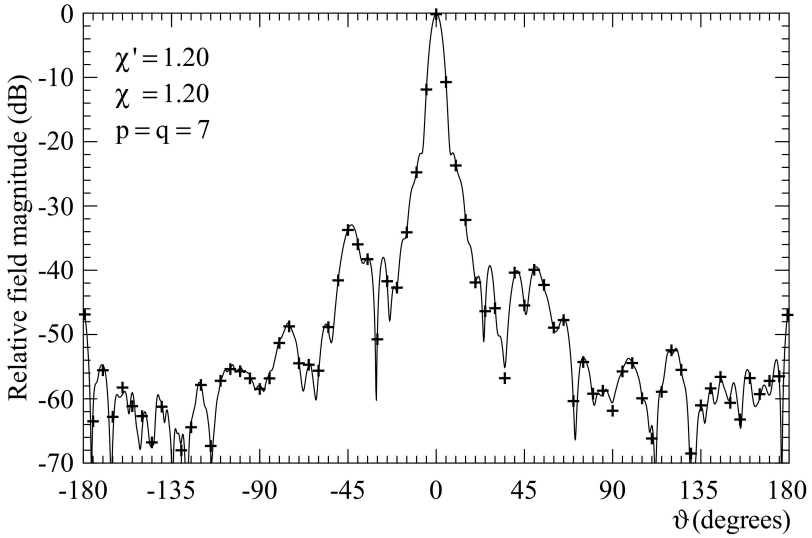

Fig. (16). H-plane pattern. Solid line: reference. Crosses: evaluated from the acquired NR NF samples.

At last, the OSI formula (12) has been used to accurately determine the NF data for the NSI-MI Technologies' software package MI-3000, implementing the CS NFTFFT [9], necessary to satisfy the minimum sphere rule in the considered offset mounting case. The so determined radiation patterns in the E- and H-planes are shown in Figs. (**15** and **16**) together with those (references) attained through the same software from the NF data directly measured on the scanning sphere. The very good agreement resulting from these FF reconstructions further confirms the validity of the proposed NR NFTFFT with spherical scan for offset mounted volumetric AUTs.

For sake of comparison, note that the number of used NR NF samples (5864) is remarkably smaller than that required by the software package MI-3000 (20200). It must be pointed out that such a number results to be also significantly smaller than the one relevant to the approach [26], requiring a NF data amount a bit greater than that (7320) used by the package MI-3000 when the AUT is onset mounted.

CONCLUSION

An effective NFTFFT for offset mounted volumetric AUTs has been developed in this paper by suitably applying the NR sampling representation to the probe voltage. It allows to drastically save measurement time, since, unlike the CS NFTFFT, it makes use of an amount of NF data minimum and equal in both the mountings in onset and offset configurations. The accuracy of the proposed NR representation and related two-dimensional OSI formula has been demonstrated both numerically and experimentally as clearly results from the very good agreement found in all the reported NF and FF reconstruction examples. The idea underling this technique will be exploited to develop NFTFFT for offset mounted AUTs whose geometry departs from the spherical one.

CONSENT FOR PUBLICATION

Not applicable.

CONFLICT OF INTEREST

The authors declare no conflict of interest, financial or otherwise.

ACKNOWLEDGEMENTS

Declared none.

REFERENCES

[1] A.D. Yaghjian, "An overview of near-field antenna measurements", *IEEE Trans. Antenn. Propag.,* vol. AP-34, pp. 30-45, 1986. [http://dx.doi.org/10.1109/TAP.1986.1143727]

[2] J. Appel-Hansen, J.D. Dyson, E.S. Gillespie, and T.G. Hickman, Antenna measurements. *The Handbook of Antenna Design.,* Peter Peregrinus: London, UK, 1986.

[3] M.H. Francis, and R.W. Wittmann, "Near-field scanning measurements: theory and practice", In: C.A. Balanis, Ed., *Modern Antenna Handbook.,* John Wiley & Sons Inc.: Hoboken, NJ, USA, 2008. [http://dx.doi.org/10.1002/9780470294154.ch19]

[4] C. Gennarelli, A. Capozzoli, L. Foged, J. Fordham, and D.J. van Rensburg, "Recent advances in near-field to far-field transformation techniques", *Int. Antennas Prop.,* vol. 2012, pp. 1-3, 2012. ID 243203 [http://dx.doi.org/10.1155/2012/243203]

[5] M.H. Francis, Ed., *IEEE Recommended Practice for Near-Field Antenna Measurements, IEEE Standard 1720-2012.*

[6] F. Ferrara, C. Gennarelli, and R. Guerriero, Near-field antenna measurement techniques.*Handbook of Antenna Technologies.,* Springer: Singapore, 2016. [http://dx.doi.org/10.1007/978-981-4560-44-3_117]

[7] A.D. Yaghjian, and R.C. Wittmann, "The receiving antenna as a linear differential operator: application to spherical near-field measurements", *IEEE Trans. Antenn. Propag.,* vol. AP-33, pp. 1175-1185, 1985. [http://dx.doi.org/10.1109/TAP.1985.1143520]

[8] J.E. Hansen, and F. Jensen, "Spherical near-field scanning at the technical university of Denmark", *IEEE Trans. Antenn. Propag.,* vol. 36, pp. 734-739, 1988. [http://dx.doi.org/10.1109/8.1174]

[9] J. Hald, J.E. Hansen, F. Jensen, and F.H. Larsen, *Spherical Near-Field Antenna Measurements.,* Peter Peregrinus: London, 1998.

[10] O.M. Bucci, C. Gennarelli, G. Riccio, and C. Savarese, "Data reduction in the NF–FF transformation technique with spherical scanning", *J. Electromagn. Waves Appl.,* vol. 15, pp. 755-775, 2001. [http://dx.doi.org/10.1163/156939301X00995]

[11] T. Laitinen, S. Pivnenko, J.M. Nielsen, and O. Breinbjerg, "Theory and practice of the FFT/matrix inversion technique for probe-corrected spherical near-field antenna measurements with high-order probes", *IEEE Trans. Antenn. Propag.,* vol. 58, pp. 2623-2631, 2010. [http://dx.doi.org/10.1109/TAP.2010.2050437]

[12] T.B. Hansen, "Spherical near-field scanning with higher-order probes", *IEEE Trans. Antenn. Propag.,* vol. 59, pp. 4049-4059, 2011. [http://dx.doi.org/10.1109/TAP.2011.2164217]

[13] F. D'Agostino, F. Ferrara, C. Gennarelli, R. Guerriero, and M. Migliozzi, "Effective antenna modellings for NF-FF transformations with spherical scanning using the minimum number of data", *Int. Antennas Prop.,* vol. 2011, pp. 1-11, 2011. ID 936781 [http://dx.doi.org/10.1155/2011/936781]

[14] T.B. Hansen, "Numerical investigation of the system-matrix method for higher-order probe correction in spherical near-field antenna measurements", *Int. Antennas Prop.,* vol. 2012, pp. 1-8, 2012. ID 493705 [http://dx.doi.org/10.1155/2012/493705]

[15] M.A. Qureshi, C.H. Schmidt, and T.F. Eibert, "Adaptive sampling in spherical and cylindrical near-field antenna measurements", *IEEE Antennas Propag. Mag.,* vol. 55, pp. 243-249, 2013. [http://dx.doi.org/10.1109/MAP.2013.6474537]

[16] F. D'Agostino, F. Ferrara, C. Gennarelli, R. Guerriero, and M. Migliozzi, "Non-redundant spherical NF – FF transformations using ellipsoidal antenna modeling: experimental assessments", *IEEE Antennas Propag. Mag.,* vol. 55, pp. 166-175, 2013. [http://dx.doi.org/10.1109/MAP.2013.6645164]

[17] F. D'Agostino, F. Ferrara, C. Gennarelli, R. Guerriero, and M. Migliozzi, "Experimental testing of nonredundant near-field to far-field transformations with spherical scanning using flexible modellings for nonvolumetric antennas", *Int. Antennas Prop.,* vol. 2013, pp. 1-10, 2013. ID 517934 [http://dx.doi.org/10.1155/2013/517934]

[18] R. Cornelius, and D. Heberling, "Spherical near-field scanning with pointwise probe correction", *IEEE Trans. Antenn. Propag.,* vol. 65, pp. 995-996, 2017. [http://dx.doi.org/10.1109/TAP.2016.2633952]

[19] R. Cornelius, and D. Heberling, "Spherical wave expansion with arbitrary origin for near-field antenna measurements", *IEEE Trans. Antenn. Propag.,* vol. 65, pp. 4385-4388, 2017. [http://dx.doi.org/10.1109/TAP.2017.2708099]

[20] F. D'Agostino, F. Ferrara, C. Gennarelli, R. Guerriero, M.A. Saporetti, F. Saccardi, L.J. Foged, and D. Trenta, "Measurement methodology for fast antenna testing using existing PNF ranges", *Proc. AMTA 2018,* 2018pp. 25-29 Williamsburg, VA, USA

[21] O.M. Bucci, and G. Franceschetti, "On the spatial bandwidth of scattered fields", *IEEE Trans. Antenn. Propag.,* vol. 35, pp. 1445-1455, 1987. [http://dx.doi.org/10.1109/TAP.1987.1144024]

[22] O.M. Bucci, C. Gennarelli, and C. Savarese, "Representation of electromagnetic fields over arbitrary surfaces by a finite and non redundant number of samples", *IEEE Trans. Antenn. Propag.,* vol. 46, pp. 351-359, 1998. [http://dx.doi.org/10.1109/8.662654]

[23] O.M. Bucci, and C. Gennarelli, "Application of nonredundant sampling representations of electromagnetic fields to NF-FF transformation techniques", *Int. Antennas Prop.,* vol. 2012, pp. 1-14, 2012. ID 319856 [http://dx.doi.org/10.1155/2012/319856]

[24] O.M. Bucci, C. Gennarelli, and C. Savarese, "Optimal interpolation of radiated fields over a sphere", *IEEE Trans. Antenn. Propag.,* vol. 39, pp. 1633-1643, 1991. [http://dx.doi.org/10.1109/8.102779]

[25] O.M. Bucci, G. D'Elia, and M.D. Migliore, "Advanced field interpolation from plane-polar samples: experimental verification", *IEEE Trans. Antenn. Propag.,* vol. 46, pp. 204-210, 1998. [http://dx.doi.org/10.1109/8.660964]

[26] L.J. Foged, P.O. Iversen, F. Mioc, and F. Saccardi, "Spherical near field offset measurements using downsampled acquisition and advanced NF/FF transformation algorithm", *Proc. EUCAP 2016,* 2016 [http://dx.doi.org/10.1109/EuCAP.2016.7481126]